

**Construction and design of an
electro-optically tunable
mode-hop free
external cavity diode laser**

Lars Levin

Master's Thesis,
LRAP 261, LTH, 2000



LUND INSTITUTE OF TECHNOLOGY
Lund University

Abstract

In frequency selective spectroscopy on cryogenically cooled materials, which might have future applications like all-optical data routing, high density optical storage, optical data rate conversion or quantum computers, it is essential to have a laser which can be tuned fast and very accurately over a bandwidth $>10\text{GHz}$. In order to fulfil these requirements an external cavity diode laser, with an intra-cavity electro-optic modulator, was designed and built. The construction builds on a novel idea, which allows fast and accurate mode-hop free frequency tuning. Mode-hop free scans extending over 10GHz have been experimentally verified. As a rigid construction is essential for the stability of the laser, much consideration was therefore given to this aspect, leading to a monolithic design.

Contents

1	Introduction.....	3
2	A system for fast, >10Ghz, sweep with high reproducibility....	3
2.1	Littrow cavity.....	3
2.2	Littrow cavity with pivot point.....	5
2.3	Electro-optic modulator inside the cavity	6
2.4	Angle compensating EOM	8
3	Characterisation of existing lasers	9
3.1	Beating against a stable reference laser	9
3.2	Analysis of the beating signal.....	10
3.3	Result.....	11
4	Description of the constructed system	12
4.1	The laser diode.....	12
4.2	Construction in Pro Engineer 2000i.....	13
4.3	Stable monolithic mechanical construction.....	13
4.4	The lens and laser diode assembly.....	14
4.5	Temperature stabilisation of the laser diode.....	14
4.6	Turning the polarisation using a $\lambda/2$ -plate.....	15
4.7	EOM crystal.....	15
4.8	Crystal and $\lambda/2$ -plate holder	15
4.9	Positioning of the crystal holder	16
4.10	Grating.....	16
4.11	Grating adjustment.....	16
4.12	Stable thermal construction	17
5	Characterisation	19
5.1	Verification of 10Ghz mode-hop free scanning	19
6	Conclusions	19
	List of symbols	21
	Abbreviations	22
	Appendix A.....	23
	Acknowledgements.....	26
	References.....	27

1 Introduction

If small amounts of a rare-earth element, for example thulium, are added when growing an otherwise transparent crystal, these ions can later be selectively excited with laser light. If the crystal is cooled down to a few degrees Kelvin, there are few vibrations disturbing the ions, and the line width of each individual ion, which is called the homogeneous line width, can become very narrow, in the case of thulium down to 3 kHz¹. However the crystal isn't perfectly regular, so different thulium ions sit in slightly different surroundings. This leads to that different ions have different absorption frequencies. For thulium this shift can be as large as 18 GHz². This means that when the ions are irradiated by a very narrow frequency laser this radiation will only interact with a very small fraction of all the ions. The fact that the ions are both spatially confined, and frequency selective, gives these crystals very interesting properties. There are many ideas of how to use these unique properties. One example is data storage with spectral hole burning³. Here one stores data by shining a laser at one specific frequency, thereby exciting all the ions that react to that frequency. If one then, at a later time, scans a laser past this point, measuring the amount of light being absorbed, a dip will be seen. The ions that are in their excited state, or removed to a meta-stable state, cause this dip.

The aim of this thesis has been to design a laser that can communicate with the ions in a crystal with properties as stated above.

Such a laser should have a narrow line width, to be able to address a specific frequency group of ions. At the same time it should be possible to frequency tune the laser over the absorption frequencies of all the different ions. A laser to be used with these crystals should meet the following specifications:

- As narrow line width, i.e. stable, as possible.
- Tunable over a large frequency interval, preferably >10GHz.
- Fast change of frequency, $\sim 1 \text{ GHz}/\mu\text{s}$.
- High reproducibility after tuning. The laser should be able to return to the same frequency after being tuned.
- High output power.

This diploma paper describes the design of an external cavity diode laser system constructed to fulfil the above specifications.

2 A system for fast, >10Ghz, sweep with high reproducibility.

In section 2.1 a basic Littrow cavity will be described. In section 2.2 and 2.3 different existing methods of tuning are outlined. Finally in section 2.4 the new tuning concept, for Littrow cavities, that was conceived and analysed during this master's thesis and its unique properties are explained.

2.1 Littrow cavity

A basic laser cavity can be constructed with a mirror, a medium that amplifies the light and a grating, see Figure 2.1.1. This is called a Littrow cavity after its designer. Such a cavity puts certain restrictions on the frequencies within it. Firstly, like in most laser cavities, the light after one roundtrip i.e. from the mirror to the grating and back to the mirror, must interfere constructively, thereby forming a standing wave, with a node on the mirror surface and nodes on the grating's grooves. If this is not the case it will interfere

destructively thereby extinguishing the light at that particular frequency. This means that the distance between the mirror and one particular groove on the grating has to be

$$L' = \frac{k\lambda}{2}, \quad (2.1.1)$$

where k is an integer, λ is the wavelength of the light, and L' is the optical length between this groove and the mirror. Note, that for the next consecutive groove $k = k + 1$ and $L' = L' + \lambda/2$, while λ is the same. The optical length of the cavity, L' , can be different from its geometrical length L . If the amplifying medium has an index of refraction $n_{am} \neq 1$ then the speed of light travelling through it is

$$v = \frac{c}{n_{am}}, \quad (2.1.2)$$

where c is the speed of light in vacuum. This means that it takes the light the same time and it experiences the same phase shift as when it travels through a distance given by

$$b' = n_{am} \cdot b \quad (2.1.3)$$

of vacuum. Here b is the geometrical length and b' is the optical length, of the amplifying medium. This is often used and referred to as optical length.

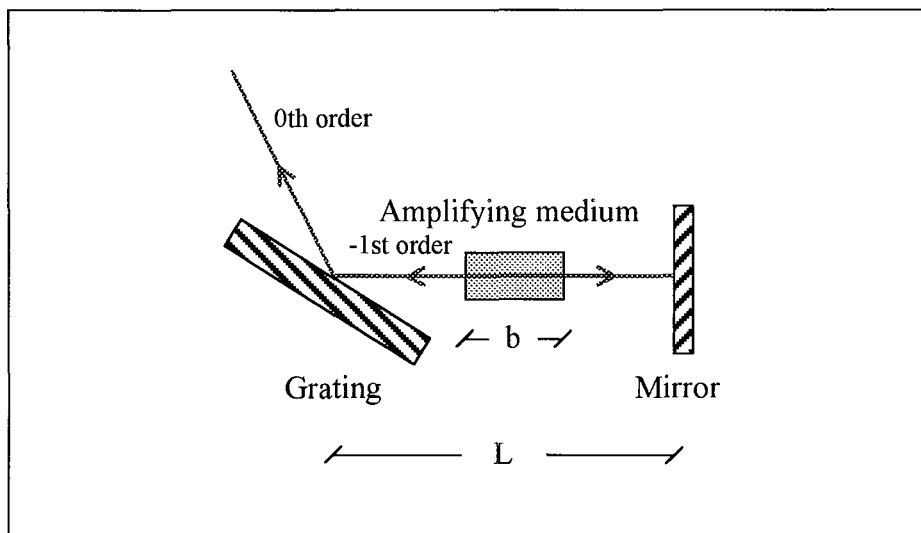


Figure 2.1.1 Basic Littrow cavity

Secondly, the distance to the next groove on the grating must be $\lambda/2$ longer, measured in the direction of the beam. Otherwise the first requirement is not fulfilled for the same wave, with k increasing by 1 for each groove, for all the grooves on the grating. The second requirement is often referred to as back coupling of the -1st order from the grating. This wavelength / frequency selective property of the grating is, of course, the reason for using it. If the grating is chosen correctly, the laser will only be lasing at one wavelength at a time. This is referred to as single mode operation.

2.2 Littrow cavity with pivot point

If one wishes to tune the frequency of the laser, it can be accomplished by moving the grating. According to the first condition in section 2.1, one roundtrip in the cavity is always an integer times the wavelength. Moving the grating back very slightly will therefore change the wavelength, but since the distance between the mirror and the grating differs from one side of the beam to the other, it has to be done with some care. The required change in cavity length, to achieve a change in wavelength of $\Delta\lambda$, can be found by differentiating equation (2.1.1), which yields

$$\Delta L' = \frac{k}{2} \Delta\lambda. \quad (2.2.1)$$

But (2.1.1) can also be rewritten as

$$\frac{k}{2} = \frac{L'}{\lambda}. \quad (2.2.2)$$

Substituting it into (2.2.1) gives

$$\Delta L' = \frac{L'}{\lambda} \Delta\lambda. \quad (2.2.3)$$

This means that to induce a certain change in wavelength $\Delta\lambda$ the movement of the grating at each point has to be proportional to the cavity length in that particular point. This can easily be accomplished by attaching the grating to an arm that has its pivot point in the elongation of the mirror's reflecting surface⁴, as shown in Figure 2.2.1. This is however not a very suitable technique when fast tuning is desired, as the grating has to be mechanically moved. If the movement is accomplished with a piezoelectric element, it also becomes difficult to return to a certain frequency due to the hysteresis of the piezo element.

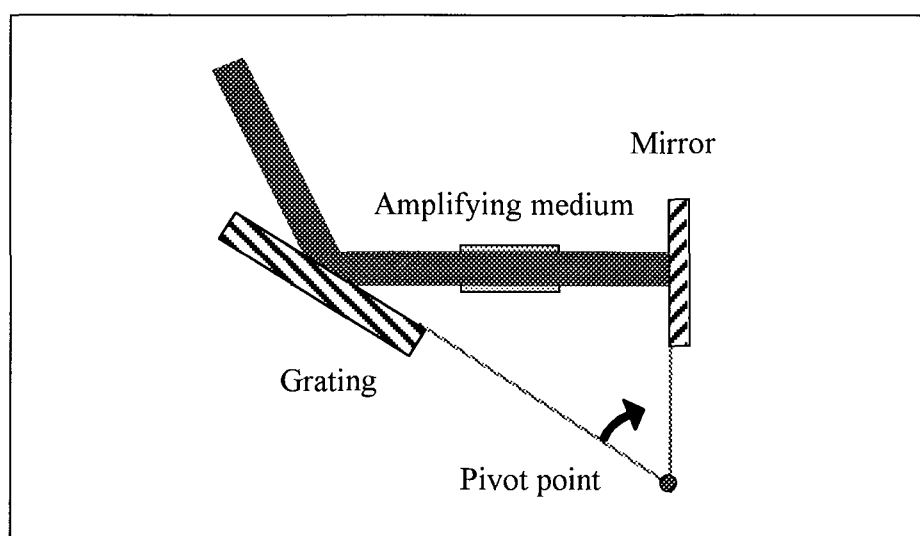


Figure 2.2.1 Pivot point for mode-hop free tuning

2.3 Electro-optic modulator inside the cavity

Some materials change their refractive index slightly when exposed to an electric field. In some cases this change is linear and is then called the linear electro-optic, or Pockel's, effect. The geometry needed to describe these changes can be somewhat complex⁵. In LiTaO₃ crystals as we have used them, it is however quite simple. If a field is applied along the optical axis, normally denoted z-direction, the light, which has its polarisation along the z-direction, will experience a change in refractive index Δn_z given by

$$\Delta n_z = -\frac{1}{2} \cdot n_z^3 \cdot r_{33} \cdot E_z. \quad (2.3.1)$$

Here $n_z = n_e$ is the extraordinary refractive index, r_{33} is the relevant element of the electro-optic tensor and E_z is the applied electric field.

The field is created by applying a voltage between two electrodes, which have been created by gold plating two sides of the crystal, as shown in Figure 2.3.1. When the voltage is applied, the E-field inside the crystal becomes

$$E_z = \frac{U}{h}. \quad (2.3.2)$$

Combining (2.3.1) and (2.3.2) yields

$$\Delta n_z = -\frac{1}{2} \cdot n_z^3 \cdot r_{33} \cdot \frac{U}{h}. \quad (2.3.3)$$

A crystal like this is normally referred to as an electro-optic modulator, EOM.

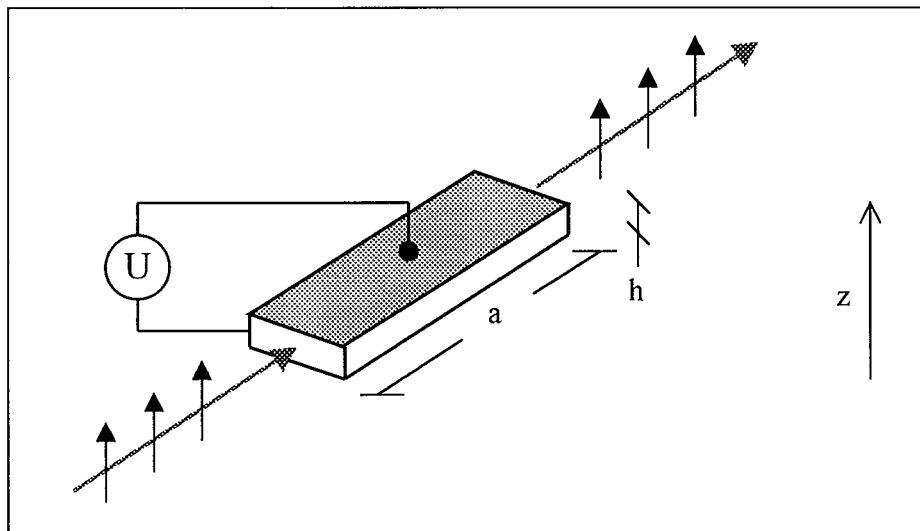


Figure 2.3.1 Electro-optic crystal with electrodes. Normally referred to as electro-optic modulator, EOM.

The length of the crystal in Figure 2.1.1 is a , and the refractive index is n_z . The change of the EOM's optical length when a voltage is applied to the electrodes becomes

$$\Delta a' = \Delta n_z \cdot a. \quad (2.3.4)$$

Equations (2.3.3) inserted into equation (2.3.4) gives

$$\Delta a' = -\frac{1}{2} \cdot n_z^3 \cdot r_{33} \cdot a \cdot \frac{U}{h}. \quad (2.3.5)$$

If the EOM is inserted into the cavity, as illustrated in Figure 2.3.2, the optical length of the cavity can be electrically tuned, thereby tuning the frequency of the laser⁶.

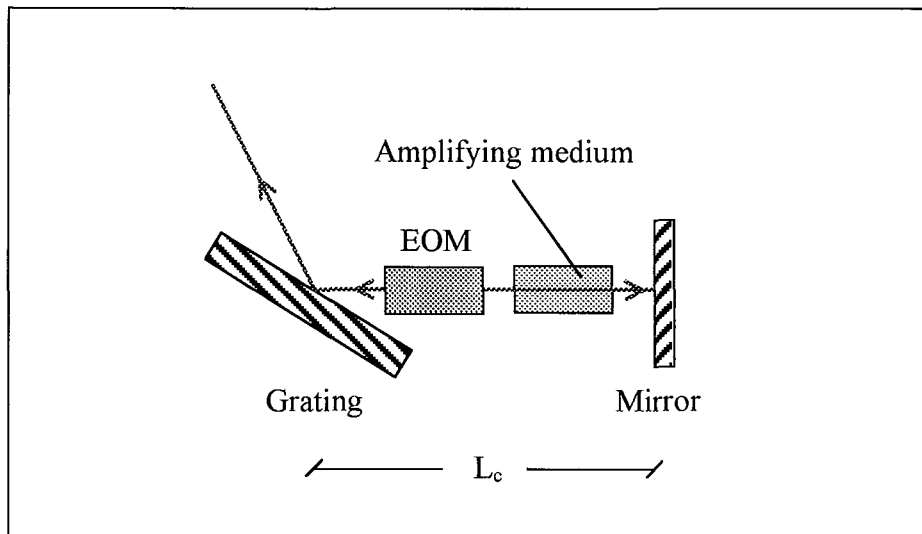


Figure 2.3.2 A laser configuration which can be frequency tuned by applying a voltage to the intra-cavity electro-optic modulator, EOM.

With this technique the frequency can be tuned very rapidly. It is also possible to achieve good reproducibility, as there is no hysteresis in the electro-optic effect of LiTaO_3 . The tuning range is however limited. In Figure 2.2.1 the tuning was done around a pivot point, thereby changing both the cavity length and the grating's angle simultaneously. Here the crystal changes only the cavity length while the feedback angle isn't changed. This is however necessary as the diffraction angle from the grating changes with the frequency. As mentioned earlier the grating has been chosen so that only one mode, the one with least losses, is lasing at any occasion. When the adjacent mode is diffracted more directly towards the mirror, this mode will experience the lowest losses and the laser mode-hops. The frequency as a function of voltage will, in principle, look something like in Figure 2.3.3.

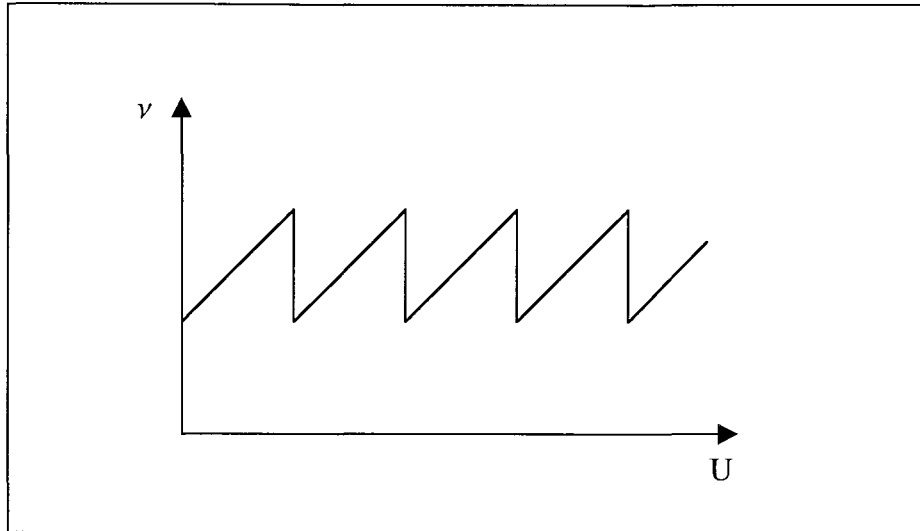


Figure 2.3.3 Laser frequency versus EOM voltage.

The maximal tunable frequency range for such a cavity is equivalent to the spacing between to consecutive modes of the cavity. This is roughly given by

$$\Delta\nu_{mode} \approx \frac{c}{2 \cdot L'_{center}}, \quad (2.3.6)$$

where L'_{center} is the optical cavity length measured at the centre of the beam. To attain as large a tuning range as possible it is therefore desirable to have a short cavity. With this construction it is however, in practice, difficult to make the cavity shorter than $\sim 5\text{cm}$, which corresponds to a maximum tuning range of

$$\Delta\nu_{mode} = \frac{c}{2 \cdot L'_{center}} = \frac{3 \cdot 10^8}{2 \cdot 0.05} = 3\text{GHz}. \quad (2.3.7)$$

A short cavity also leads to large instantaneous line width if there are any mechanical instabilities in the cavity. The reason for this is that a fractional change in cavity length results in the same fractional change of the laser frequency. Hence with a short cavity length, a very small cavity length change will result in a sizeable frequency shift.

2.4 Angle compensating EOM

The two earlier described methods of tuning a Littrow cavity both have their virtues. Tuning by turning the grating around a well-chosen pivot point gives large mode-hop free tuning range and the intra-cavity EOM method offers fast tuning with high reproducibility. In the novel design described below, these qualities are combined.

The mode-hop free tuning in section 2.2 was obtained by letting the cavity's elongation be proportional to the cavity's length in each particular point. With the intra-cavity electro-optic modulator design, the change of optical length of the cavity is achieved by altering the refractive index of the EOM by applying an electric field across it. The field is, for a certain applied voltage and crystal length, inversely proportional to the crystal's thickness, b . By letting the crystal's thickness vary across the beam, as in Figure 2.4.1, one can

achieve the proportional elongation that is required for mode-hop free tuning. The method for calculating the proper angle of the crystal is shown in Appendix A.

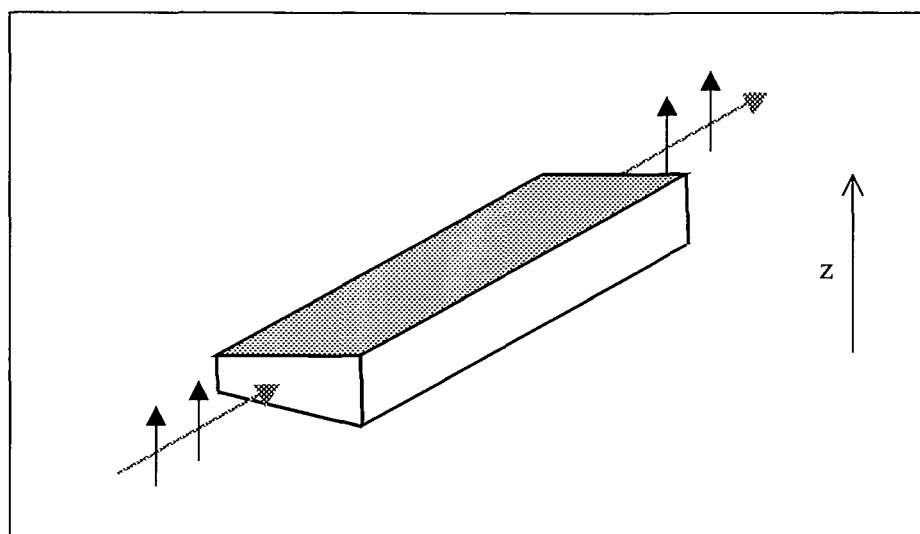


Figure 2.4.1 Crystal with angled sides.

3 Characterisation of existing lasers

As was explained in the Introduction another important feature of the laser is the stability of the output frequency (the line width). In order to determine what is needed to minimise the line width, measurements were made of the output frequencies on two existing external cavity diode lasers, (ECDL).

3.1 Beating against a stable reference laser

A simple way of measuring the frequency of a laser is by heterodyne mixing it with a stable reference laser, as shown in Figure 3.1.1.

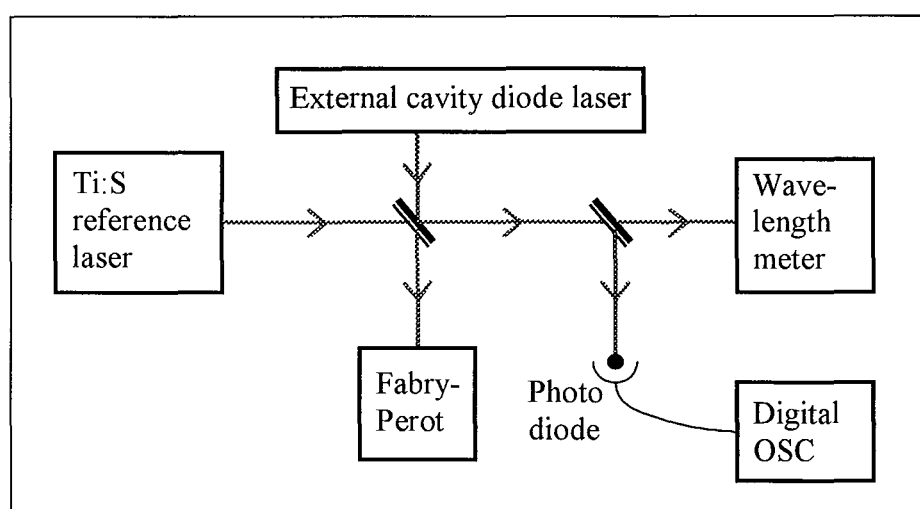


Figure 3.1.1 Experimental set-up for measurement of the laser frequency by heterodyne beating against a stable reference laser.

The reference laser was a Microlase model MBR-110 Ti:S laser, with a line width around 100kHz. When the radiation from this and one of the lasers to be evaluated are mixed on the photodiode, Electro-Optics Technology ET 2010, an amplitude modulation equal to the difference in frequency of the two lasers can be measured. The frequencies of the lasers are adjusted to coincide in two steps. Firstly they are set to approximately the same value with the wavelength meter. Then they are brought closer together by watching the fringes of a scanning Fabry-Perot etalon, Coherent model 240-2-B, 1.5GHz free spectral range. After these two steps their frequencies are close enough for the beating to be registered by the oscilloscope, Tektronix TDS 540, 500 Mhz.

3.2 Analysis of the beating signal

The frequency of the beating can be determined using fast Fourier transforms, (FFT). It is, however, of interest to know how the frequency changes with time. Therefore long beat sequences, typically 50 000 data points, were collected and then analysed with windowed Fourier transforms. The principle of this is that one cuts out a piece of the data, for example 1024 data points, multiplies it by a window function, to avoid effects of the sharp sides edges at the start and at the end of the 1024 bit long sequence, and then determines the frequency of this piece with FFT. Next one moves slightly forward, for example 100 data points, and repeats the procedure. This gives a sequence of frequency spectra, in our example 500, for successive times. These are density plotted after each other which finally yields a diagram like that shown in Figure 3.2.1.

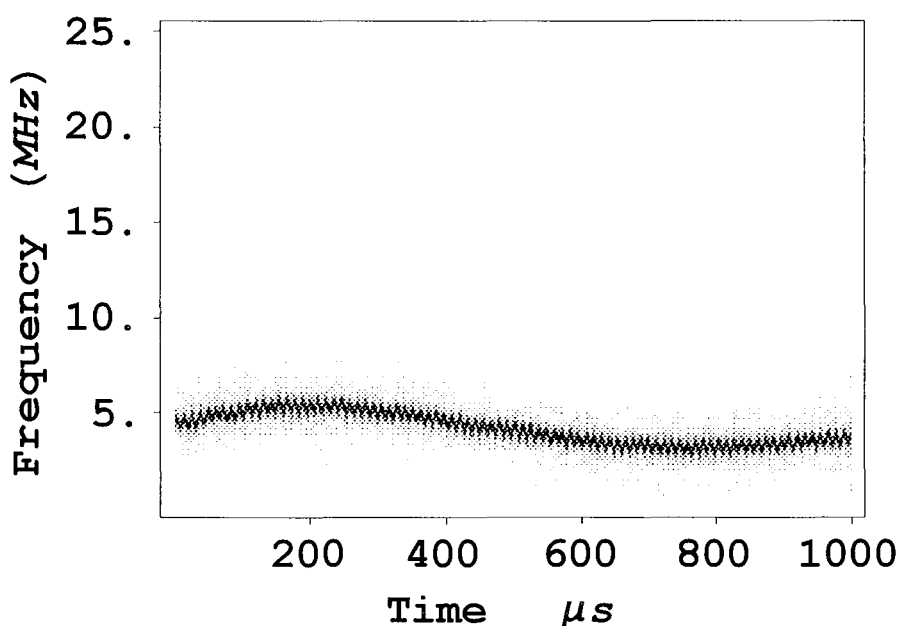


Figure 3.2.1 Windowed Fourier transform of the beating between a stable reference laser and a ECDL.

The small frequency oscillations which are seen in Figure 3.2.1 originates from the frequency locking system on the Ti:S reference laser. The Ti:S laser is locked against the transmission fringe from an internal Fabry Perot cavity. This is done by slightly varying the frequency of the laser, while monitoring the change in transmission through the cavity. Another phenomenon which might need explaining, is the folding that occurs when the beating frequency exceeds half of the sampling frequency, which is equal to the maximum frequency that can be unambiguously measured. This is illustrated in Figure 3.2.2, where

the intra-cavity EOM and has a much stiffer mechanical construction. In Figure 3.3.1 it is clearly seen that laser B, which has a more rigid construction, is at least a factor 10 more stable than laser A. This, together with the fact that the frequency changes are quite slow, leads us to the conclusion that the mechanical stability of the laser is of utmost importance.

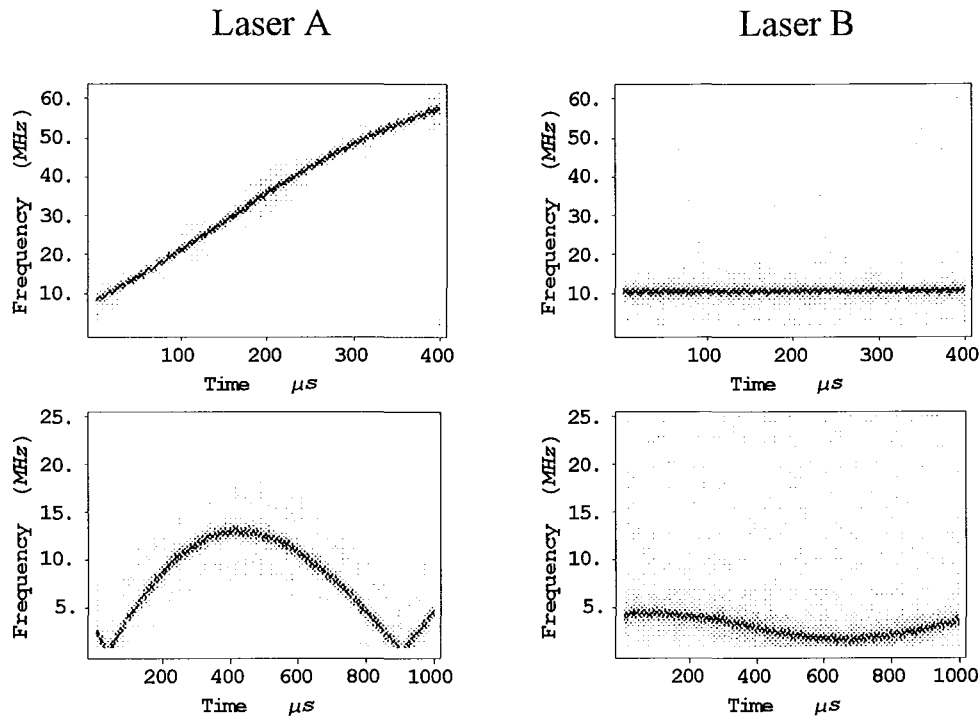


Figure 3.3.1 Results from beating laser A and laser B against the Ti:S reference laser.

4 Description of the constructed system

In addition to what has been mentioned earlier, we will here go through the actual laser construction, trying to emphasise what components were used and why.

4.1 The laser diode

Traditionally the gain medium in Littrow cavities has often been an externally pumped dye-cell or -jet. This requires a pump laser and a dye system, which is quite costly and complicated. Therefore the use of laser diodes as a gain medium has become very popular^{8,9}. The laser diode is incorporated into the cavity as shown in Figure 4.1.1. When manufactured, the back facet (right hand side in Figure 4.1.1) of the laser diode chip is generally coated in order to get high reflectivity. This side is used as the end mirror of the external cavity. The front facet (left side) is normally not coated when the diode is made, which leads to a reflectivity of $\sim 30\%$ since the refractive index of the diode is ~ 3.5 ¹⁰. If this side is left uncoated, the laser diode will act as an etalon and interference in this etalon will hinder smooth tuning. Therefore the facet is anti-reflection coated to give a residual reflectivity of $< 1 \cdot 10^{-4}$ ¹¹.

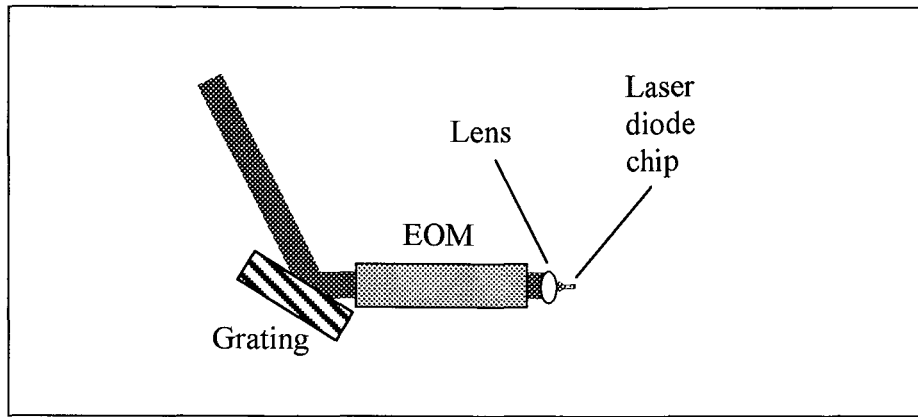


Figure 4.1.1 External cavity diode laser.

It is desirable to have sufficiently high output power combined with a good spatial mode. Therefore the market was thoroughly investigated to find a single spatial mode diode laser with as high output power as possible. Finally a SDL-5311-G1 diode, anti-reflection coated by Sacher Lasertechnik was chosen. When Sacher sells this diode they call it SAL-795-50. The laser diode has, before the anti-reflection coating was done, a stand alone output power of 100mW, and it should be possible to achieve 50mW when used with an external cavity. The diode was driven by a Profile LDC 202 diode controller. If one in the future, wishes to reach even higher output power, there are several promising methods. One of them is the amplification of the signal by letting it pass through a second laser diode¹²⁻¹⁵.

4.2 Construction in Pro Engineer 2000i

In order to construct and manufacture the different components with the required accuracy, the whole laser was designed with the CAD/CAM software PRO/ENGINEER 2000i. The code for the numerically controlled milling machine was then generated directly from the Pro E model. The pictures in the following sections are taken from Pro E.

4.3 Stable monolithic mechanical construction

In order to achieve a construction which is as rigid as possible, a monolithic aluminium design was chosen. In practice this means that a pocket was milled in a solid block of aluminium, and on or within the walls of this pocket, the laser diode, grating and the other components were mounted. This construction is very stiff, which leads to a low vibration level. Figure 4.3.1 shows the monolith from two different angles.

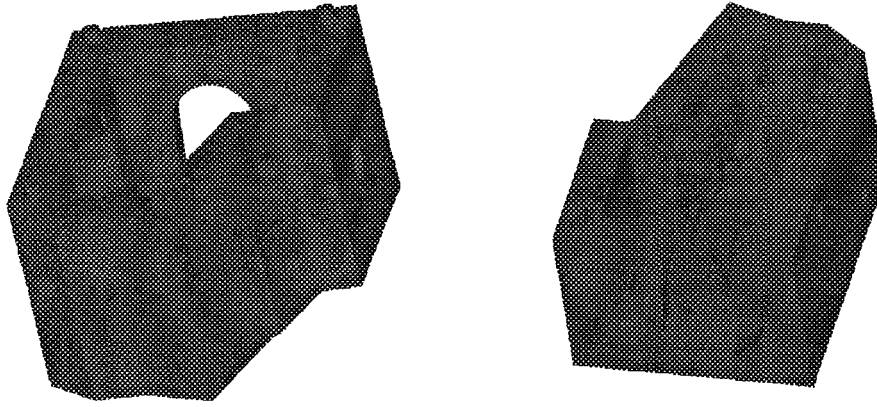


Figure 4.3.1 Aluminium monolith showed from two different angles.

4.4 The lens and laser diode assembly

To allow simple and stable focusing, the lens in its housing, Thorlabs LT230P-B, and the laser diode, Sacher Lasertechnik SAL-795-50, was mounted in a collimation tube, Thorlabs C330TM-B. The collimation tube is threaded and the lens is screwed into the collimation tube. The distance between the lens and the diode is adjusted by turning the lens. To be able to turn the lens, after assembling the laser, a cogwheel, taken from an old ABC 80 printer, was glued to the lens¹⁶. In Figure 4.4.1 the collimation tube with the lens mounted is shown.

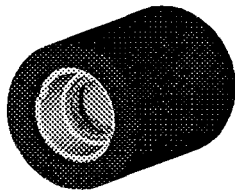


Figure 4.4.1 Collimation tube with mounted lens.

4.5 Temperature stabilisation of the laser diode

The diode laser needs to be temperature controlled, as its characteristics is highly temperature dependent. This is done with a temperature controller, Profile TED 200. However one often wishes to utilise this temperature dependence while adjusting the laser. Therefore it is preferable to have a small thermal mass, to be controlled together with it. In order to achieve this the collimation tube was thermally connected to a Peltier element, Melcor OT2.0-66-F0, with a small copper wedge, shown in Figure 4.5.1 a. The heat from the other side of the Peltier element was led away to the base plate through a copper braid, to minimise the vibration transfer. The temperature was measured with an IC temperature transducer, Analog devices AD 592 CN, mounted in the hole, which can be seen on the front of the wedge. All of these components were thermally isolated from the monolith by mounting them in a block of G10 fibreglass, which is shown in Figure 4.5.1 b. This material was chosen because that it leads heat poorly, while at the same time being very rigid.

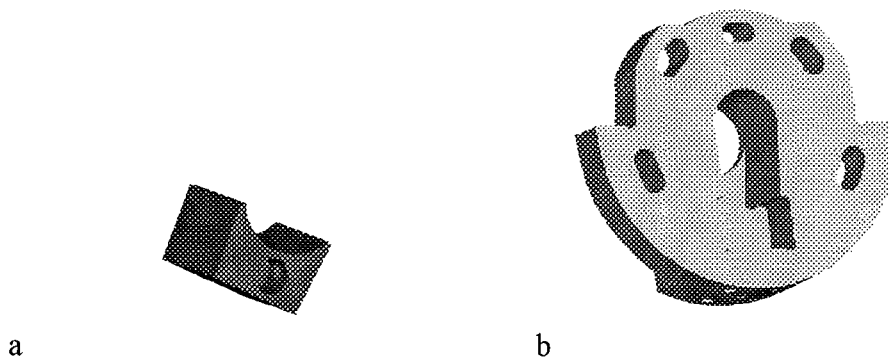


Figure 4.5.1 In part a the Copper wedge used to thermally connect the collimation tube to the Peltier element is shown. Part b shows the G10 plate in which the collimation tube, copper wedge, Peltier element and one end of the copper braid was mounted.

4.6 Turning the polarisation using a $\lambda/2$ -plate

As it is difficult to manufacture a grazing incidence grating with high efficiency for beams with the polarisation perpendicular to the grating's grooves¹⁷, the polarisation was rotated 90 degrees, in-between the crystal and the grating by inserting a $\lambda/2$ -plate, Casix WPF 1215 $\lambda/2$ -plate. To avoid any intra-cavity etalon effects, the $\lambda/2$ -plate was tilted 8 degrees.

4.7 EOM crystal

The EOM crystal, 40 x 15 x 1-1.5mm, was made of LiTaO₃. The electrodes were created by gold plating to of its sides, leaving a 1mm border at the edges, to decrease the risk for an electrical discharge between the electrodes. The two end facets were anti-reflection coated to yield a residual reflectivity of <0.1%. The crystal and coatings were custom made to our specifications by Casix.

4.8 Crystal and $\lambda/2$ -plate holder

A special holder was manufactured for mounting the crystal and the $\lambda/2$ -plate. As the holder should be stable, and at the same time be electrically isolating, it was made of G10 epoxy glass fibre. The holder was made in two halves. Each half has a groove, in which the wire for applying the high voltage resides. The end of the wire was soldered to a thin (0.05mm) copper plate, which served as contact to the gold electrodes. At the end of the holder a tilted seat was made in which the $\lambda/2$ -plate was mounted. In Figure 4.8.1 the two halves of the crystal holder, and the assembled holder with the $\lambda/2$ -plate mounted is shown.

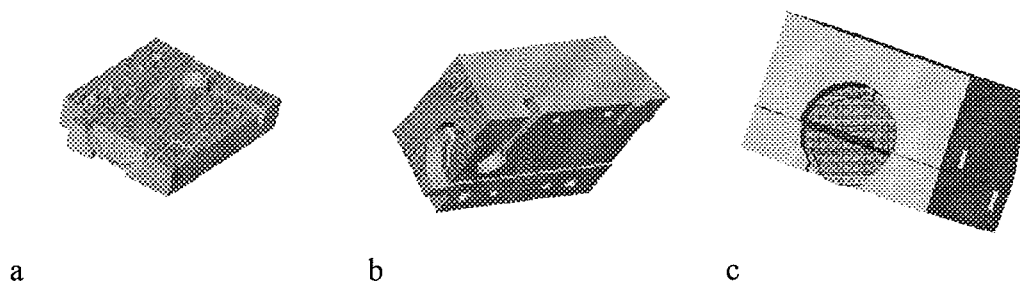


Figure 4.8.1 Crystal holder. Part a, bottom half, part b top half and part c assembled with the $\lambda/2$ -plate mounted.

4.9 Positioning of the crystal holder

Fine-tuning of the matching between the angle deviation and the elongation of the cavity is achieved by moving the crystal sideways. To this end the crystal holder was mounted on a positioning stage, Del-Tron 101XM. To allow proper placement of the crystal in the beam path the positioning stage was screwed to a locally manufactured aluminium plate, which could be adjusted, with three hex adjustment screws, Thorlabs F25SS-075. The adjustment screws were mounted in brass bushings, Thorlabs N80L5. The plate was held down against the monolith with two hard springs. Figure 2.1.1 shows the plate with the adjustment screws and the bushings.

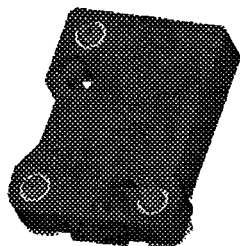


Figure 4.9.1 Crystal holder plate with hex adjustment screws.

4.10 Grating

In order to get a high dispersion, and at the same time illuminating as many grooves as possible, a gold coated grating with 2400 grooves/mm, Spectrogon L2400 custom design, was chosen. The feedback efficiency for the grating in Littrow configuration was specified to be 20% at $\lambda = 793\text{nm}$.

4.11 Grating adjustment

The grating was mounted in a locally manufactured holder, shown in Figure 4.11.1. Turning the grating sets the working wavelength of the laser. This is however a delicate business, and therefore high quality sub-micron adjusters, Thorlabs MDT216, were chosen. The preliminary tests seem to indicate that this was a god choice. The third corner of the holder was controlled with a hex screw, Thorlabs F25SS-100, mounted in a brass bushing, Thorlabs N80L7. The whole grating holder was pushed against the monolith wall with two stiff springs, found on the pavement while strolling to lunch.

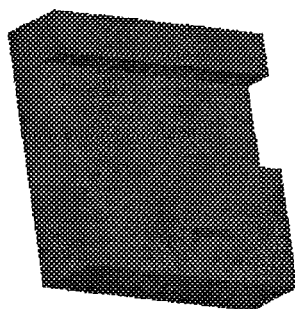


Figure 4.11.1 Grating holder.

4.12 Stable thermal construction

The change in wavelength corresponding to a certain change in frequency is given by

$$\Delta\lambda = -\frac{\lambda^2}{c} \cdot \Delta\nu. \quad (4.12.1)$$

Equation (2.2.3) can be rewritten to give the change in wavelength as a function of change in cavity length. If these two equations are combined one gets

$$\Delta\nu = -\frac{c}{L' \cdot \lambda} \cdot \Delta L'. \quad (4.12.2)$$

If the temperature of the cavity changes by an amount ΔT , the length of it will change according to

$$\Delta L' = L \cdot \alpha_{Al} \cdot \Delta T, \quad (4.12.3)$$

where $L \approx 0.06\text{m}$ is the geometrical length of the cavity and $\alpha_{Al} = 2.4 \cdot 10^{-5} \text{ 1/K}$ is the linear thermal expansion coefficient. Combining equation (4.12.2) and (4.12.3), and inserting approximate values for our laser yields

$$\begin{aligned} \Delta\nu &= -\frac{c}{L' \cdot \lambda} \cdot L \cdot \alpha_{Al} \cdot \Delta T \\ &= \frac{3 \cdot 10^8}{0.11 \cdot 793 \cdot 10^{-9}} \cdot 0.06 \cdot 2.4 \cdot 10^{-5} \cdot \Delta T \\ &\approx 5 \cdot 10^9 \Delta T. \end{aligned} \quad (4.12.4)$$

That is 5GHz/K. This means that the temperature of the monolith has to be stabilised with a temperature controller¹⁸ to minimise the frequency fluctuations. The temperature is measured with a second IC temperature transducer, Analog devices AD 592 CN, mounted in a hole in the bottom of the monolith. The temperature of the hole monolith was controlled by inserting 4 Peltier elements, Supercool PE-071-14-11-S, between the monolith and the base plate. The rest of the base plate, and the connections plate, was covered with thermal insulation, Armstrong AP Armaflex. The thermal insulation sheets are pointed out with arrows in Figure 4.12.1. To thermally shield the whole construction, a cover with insulation on the inside was then placed over it. In Figure 4.12.2 the laser is shown with the cover assembled.

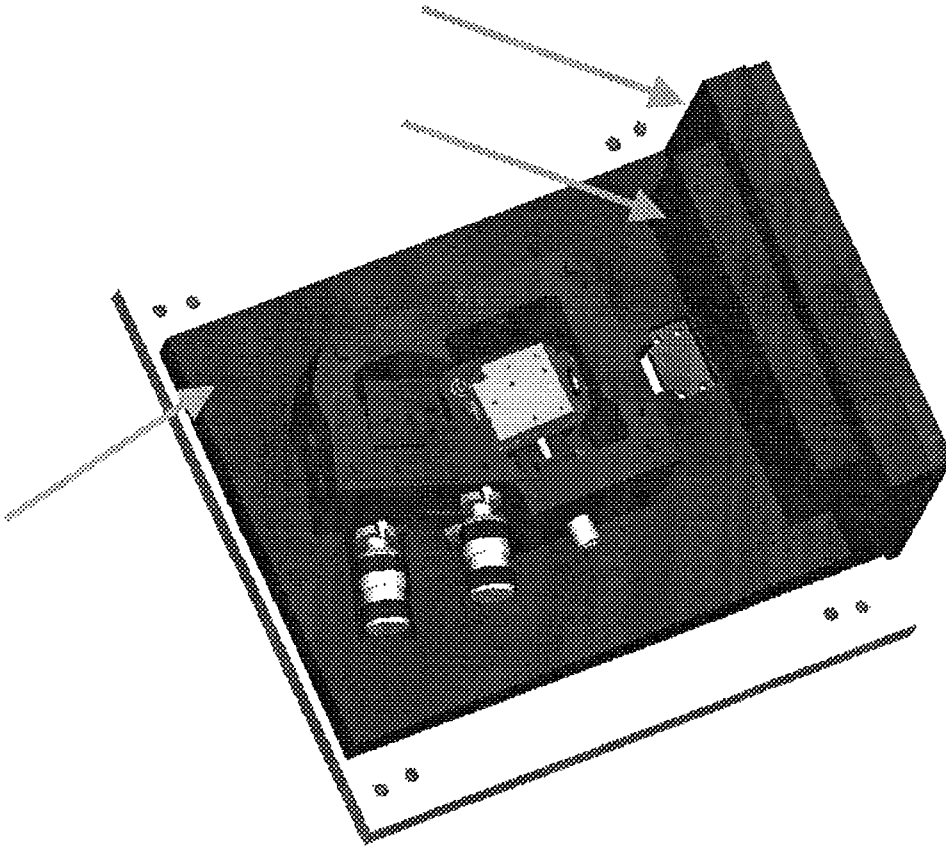


Figure 4.12.1 Laser with cover removed.

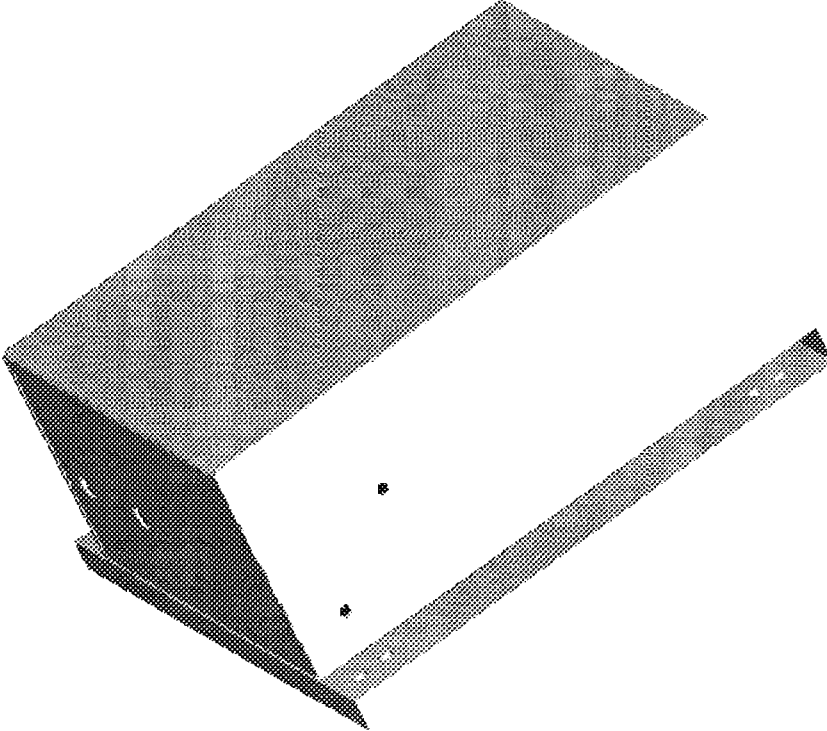


Figure 4.12.2 Laser with mounted cover.

5 Characterisation

The aim of this master's thesis has been the design and construction of the laser. Extensive characterisation and testing will be performed after this thesis, and the only testing done so far is the verification of the extended, mode-hop free scanning range.

5.1 Verification of 10GHz mode-hop free scanning

In order to check this a 0 – 1.9 V ramp was created using a synthesised function generator, Stanford Research Systems DS 345, which was used to control a high voltage source, Stanford Research Systems PS 350, to generate an output ramp of 0 – 950V. This ramp was then fed through a protecting circuit, which approximately let through 80% of the voltage, to the EOM crystal. The output wavelength from the laser was then measured with a wavelength meter, Burleigh WA-4500. The wave meter calculates the wavelength of the laser for each acquisition. In Figure 5.1.1 these values have been drawn against the calculated EOM voltage. This scan exceeds 10GHz, but larger scans should be possible after the adjustment of the laser.

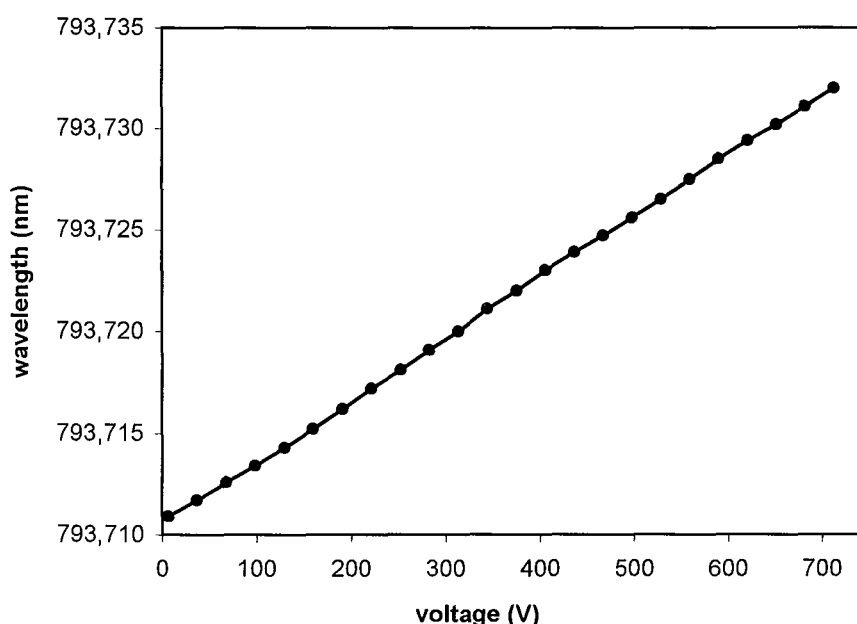


Figure 5.1.1 Laser output wavelength versus calculated EOM voltage.

6 Conclusions

After the test and evaluation of existing external cavity diode lasers, an intra-cavity electro-optically tunable laser was built with a novel design, which allows mode-hop free tuning. Mode-hop free tuning over 10 GHz was then experimentally verified. The tests conducted on existing lasers also revealed that a stable mechanical construction was of utmost importance for the frequency stability and scanning reproducibility of the laser. Therefore a monolithic design was chosen, and we are looking forward to future measurements on the stability and the improved experiments that this might allow. We also look forward to verifying the fast change of frequency, which we expect to be of the order of several GHz/ μ s. To obtain high output power, combined with good spatial mode

quality a powerful single mode laser diode was chosen, which should allow an output power of 30-50mW. However, for some experiments even higher power is required and a very interesting future extension would be the amplification of the beam by it sending it through a broad area diode laser, which then acts as a laser power amplifier. Power amplification in the order of ten times has been shown for such systems working at 805nm¹³, and similar laser diodes are available at 793nm. The laser can be seen in Figure 6.1 and Figure 6.2.

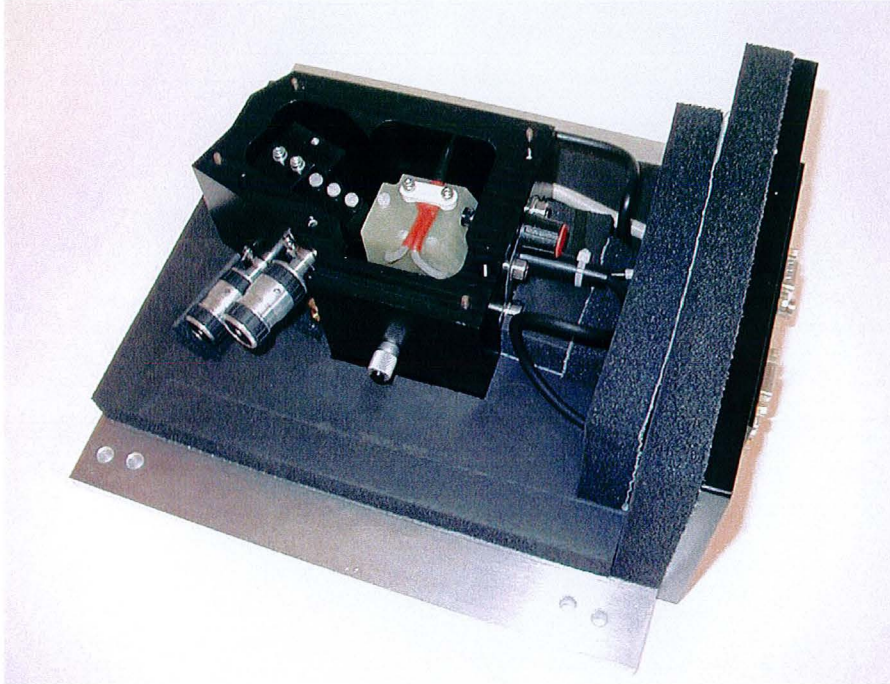


Figure 6.1 Picture of the laser with the cover off.

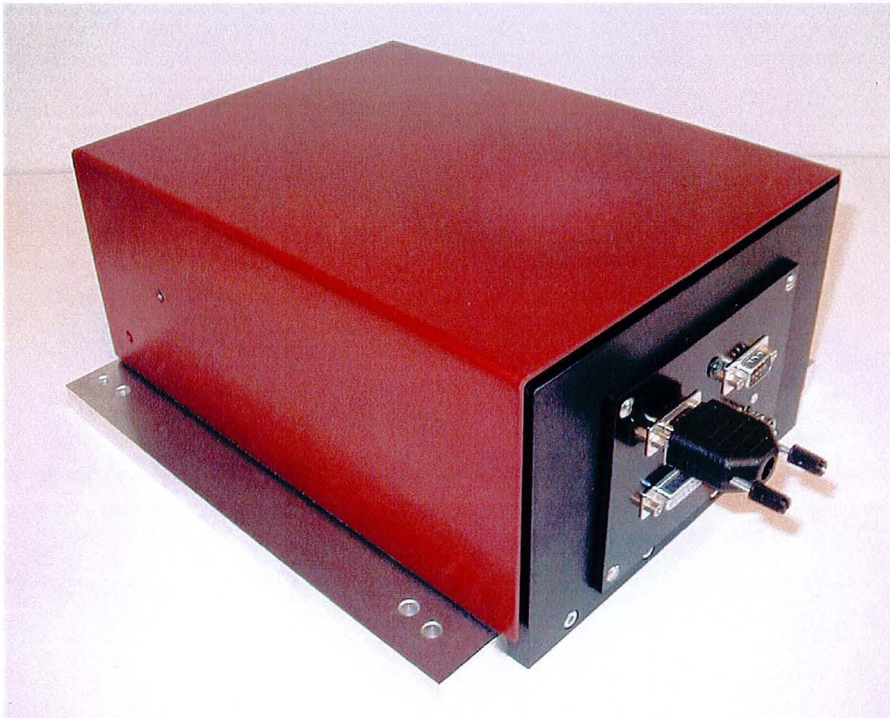


Figure 6.2 Picture of the laser with the cover on.

List of symbols

a	=	The electro-optic crystal length, measured along the beam path.
a'	=	The electro-optic crystal optical length, measured along the beam path.
c	=	The speed of light in vacuum.
C_1	=	$\frac{1}{2} \cdot n_z^3 \cdot r_{33}$
d	=	The groove spacing of the grating.
E_z	=	Electric field applied across the electro-optic crystal.
f_{obs}	=	The observed frequency.
f_{samp}	=	The sampling rate.
f_{true}	=	The actual beat frequency.
h	=	Crystal thickness.
h_{center}	=	Crystal thickness measured at the centre of the beam.
k	=	Number of wavelengths for one roundtrip in the cavity. This is different for each particular groove.
L	=	Geometrical cavity length. This is different for different sides of the cavity.
L'	=	Optical cavity length. This is different for different sides of the cavity.
L'_{center}	=	Optical cavity length measured at the centre of the beam.
n_{am}	=	Index of refraction of the amplifying medium.
n_z	=	n_e = Extraordinary refractive index. For LiTaO ₃ $n_e = 2.16$ at 793nm ¹⁹ .
r_{33}	=	Element in the electro-optic tensor. For LiTaO ₃ $r_{33} = 30.4 \cdot 10^{-12} \text{ m/V}^{20}$.
U	=	Voltage applied between the electrodes of the electro-optic crystal.
α_{Al}	=	$2.4 \cdot 10^{-5} \text{ K}^{-1}$. Coefficient of linear thermal expansion for aluminium.
$\Delta a'$	=	Change in the optical length of the electro-optic crystal due to an applied field.
$\Delta L'$	=	Change in the optical cavity length.
Δn_z	=	Change in index of refraction due to applied field.
$\Delta \beta$	=	Beam deflection angle, caused by the crystal.
$\Delta \gamma$	=	Change in γ due to changing wavelength.
$\Delta \lambda$	=	Change in wavelength.
$\Delta \nu$	=	Change of frequency.
$\Delta \nu_{mode}$	=	Frequency distance between two consecutive cavity modes.
γ	=	Angle of incidence onto the grating. For Littrow configuration this equals the angle of diffraction.
λ	=	Wavelength.

Abbreviations

EOM	=	Electro-optic modulator, section 2.3
ECDL	=	External cavity diode laser, section 3
FFT	=	Fast Fourier transform, section 3.2
IC	=	Integrated circuit, section 4.5

Appendix A

In order to calculate the angle of a crystal to be used in a mode-hop free Littrow cavity we first consider what happens when a plane wave impinges on a crystal with sideways changing index of refraction. Such a wave will experience different refractive indices across its cross section. This causes the wave to tilt and leave the crystal at an angle^{21,22}, as illustrated in Figure A.1.

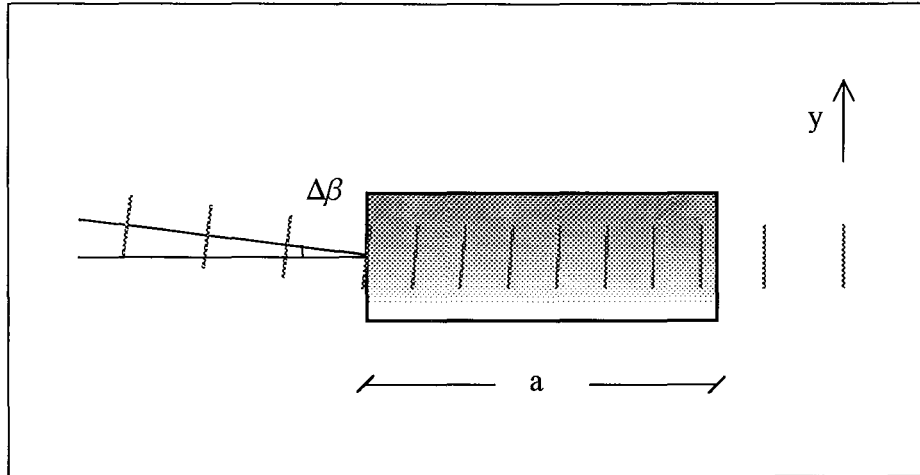


Figure A.1 Propagation of a plane wave through a crystal where the index of refraction increases as a function y , causes the beam to deflect an angle $\Delta\beta$.

If the refractive index changes are small, the deflection angle is given by²¹

$$\Delta\beta = a \cdot \frac{\partial}{\partial y} (\Delta n_z), \quad (\text{A.1})$$

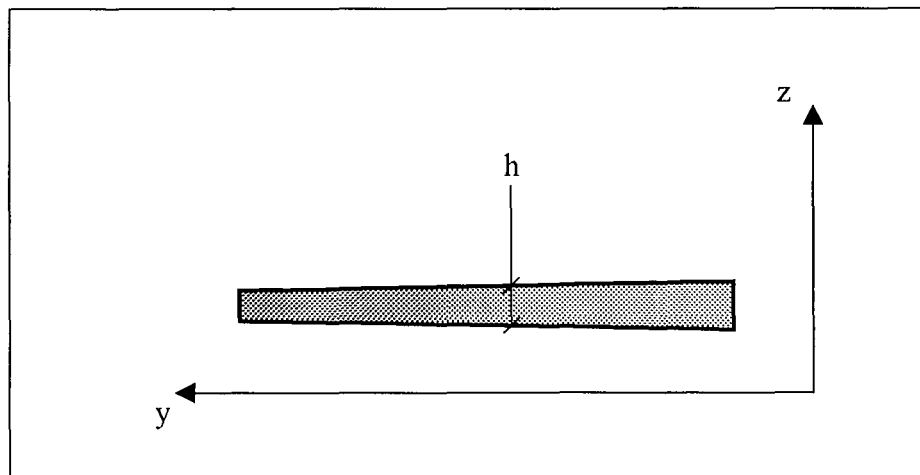


Figure A.2 Crystal with slowly varying cross section.

For a crystal with slowly varying cross-section, as shown in Figure A.2 $\frac{\partial}{\partial y}(\Delta n_z)$ can be calculated from equation (2.3.3) and yields

$$\frac{\partial}{\partial y}(\Delta n_z) = -C_1 \cdot U \cdot \frac{\partial}{\partial y}\left(\frac{1}{h}\right) = C_1 \cdot U \cdot \frac{1}{h^2} \frac{\partial h}{\partial y}, \quad (\text{A.2})$$

where $C_1 = \frac{1}{2} \cdot n_z^3 \cdot r_{33}$. Combining equation (A.1) with equation (A.2) gives the exit angle as

$$\Delta\beta = a \cdot C_1 \cdot U \cdot \frac{1}{h^2} \frac{\partial h}{\partial y}. \quad (\text{A.3})$$

The change in the wavelength of the laser, according to equation (2.2.3), is

$$\Delta\lambda = \frac{\lambda}{L'} \Delta L'. \quad (\text{A.4})$$

The change in the cavity length, when the field is applied, according to equation (2.3.5), is

$$\Delta L' = \Delta a' = -C_1 \cdot a \cdot \frac{U}{h}. \quad (\text{A.5})$$

At the centre of the beam this yields

$$\Delta\lambda = -\frac{\lambda}{L'_{center}} \cdot C_1 \cdot a \cdot \frac{U}{h_{center}}. \quad (\text{A.6})$$

This change in wavelength will change the perfect angle of feedback from the grating, γ . When the feedback conditions are perfect, the distance between two consecutive grooves is $\lambda/2$, measured in the direction of the beam as shown in Figure A.3. This means that

$$\lambda = 2 \cdot d \cdot \sin(\gamma), \quad (\text{A.7})$$

where d is the distance between two consecutive grooves. In order to calculate how much the angle changes when the wavelength is shifted, equation (A.7) is differentiated, which gives

$$\Delta\gamma = \frac{1}{2 \cdot d \cdot \cos(\gamma)} \cdot \Delta\lambda, \quad (\text{A.8})$$

where γ can be calculated from equation (A.7). Inserting equation (A.6) into equation (A.8) yields

$$\Delta\gamma = -\frac{1}{2 \cdot d \cdot \cos(\gamma)} \cdot \frac{\lambda}{L'_{center}} \cdot C_1 \cdot a \cdot \frac{U}{h_{center}}, \quad (\text{A.9})$$

This change of angle should be compensated for by the alteration of the angle out from the crystal, $\Delta\beta$, given by equation (A.3), with leads to

$$\begin{aligned} \Delta\gamma &= \Delta\beta \Rightarrow \\ -\frac{1}{2 \cdot d \cdot \cos(\gamma)} \cdot \frac{\lambda}{L'_{center}} \cdot C_1 \cdot a \cdot \frac{U}{h_{center}} &= \\ a \cdot C_1 \cdot U \cdot \frac{1}{h_{center}^2} \frac{\partial h}{\partial y} &\Rightarrow \\ -\frac{\lambda}{L'_{center} \cdot 2 \cdot d \cdot \cos(\gamma)} &= \frac{1}{h_{center}} \frac{\partial h}{\partial y}. \end{aligned} \quad (\text{A.10})$$

This can finally be rewritten as

$$\frac{\partial h}{\partial y} = -\frac{\lambda}{2 \cdot d \cdot \cos(\gamma)} \cdot \frac{h_{center}}{L'_{center}}, \quad (\text{A.11})$$

where γ can be calculated from equation (A.7).

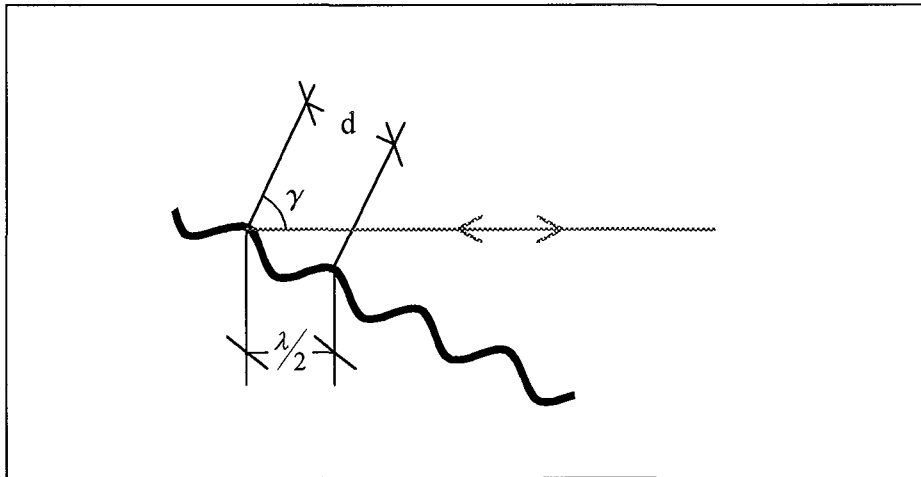


Figure A.3 Grating feedback condition. The wiggly line is the grating surface, d is the spacing between the grooves and γ is the angle between the beam and the grating normal.

Acknowledgements

This project would not have been possible, or half as fun, without the enthusiastic help I have received from so many people. I would like to express my sincere gratitude to all who supported me, especially to:

Stefan Kröll, my tutor, who I chose to do my diploma work with, after having him as teacher, where he possessed the rare quality of answering the actual questions put to him, not the questions he expected. Thanks for all the enthusiastic help and support during this work, and for your way of always being open to new ideas.

Krishna Mohan, for always taking time off to answer all my questions and for all the interesting discussions about diode lasers and everything else.

Kjell Lundman, division of production and material engineering, for, in the most hospitable way, showing me how to operate a numerically controlled milling machine.

Nicklas Ohlsson for straightening out my understanding of the systems we work with, and everything else.

Jan Hultqvist, for the excellent help with manufacturing some of the parts, and Göran Werner and everybody else in the workshop for helping me out in all situations.

Åke Bergquist, for all the help with the electronics, and together with Bertil Hermansson, making sure that I felt welcome to the department.

Anders Larsson, who helped me with the E-field of the crystal.

Jonas Sandsten and Ulf Gustafsson, for their friendly help with questions regarding diode lasers.

Sven Spanne and Gunnar Sparr, centre for mathematical sciences, for their input on the analysis of the beat signals.

Elsie Nilsson, for making sure that I had enough coffee.

To everyone else in the division, especially, Laila Lewin, Claes-Göran Wahlstöm, Anders Persson, Petter Weibring, Britt-Marie Hansson and Marie Holmdahl-Svensson.

Sune Svanberg who inspired me to study atomic physics.

My family, for all your support during the whole of my education.

Finally and mostly I want to thank my girlfriend, Catarina, and my daughter Freja, for all your love.

References

1. Macfarlane, R. M., Photon-Echo Measurements On the Trivalent Thulium Ion, *Optics Letters* **18**, 1958-1960 (1993).
2. Greiner, C., Boggs, B., Loftus, T., Wang, T. & Mossberg, T. W., Polarization-dependent Rabi frequency beats in the coherent response of Tm³⁺ in YAG, *Physical Review A* **60**, R2657-R2660 (1999).
3. Maniloff, E. S., Johnson, A. E. & Mossberg, T. W., Spectral data storage using rare-earth-doped crystals, *MRS Bulletin* **24**, 46-50 (1999).
4. Trutna, W. R. & Stokes, L. F., Continuously Tuned External-Cavity Semiconductor-Laser, *Journal of Lightwave Technology* **11**, 1279-1286 (1993).
5. Boyd, R. W., *Nonlinear optics*, (Academic press limited, London, England, 1992).
6. Greiner, C., Boggs, B., Wang, T. & Mossberg, T. W., Laser frequency stabilization by means of optical self-heterodyne beat-frequency control, *Optics Letters* **23**, 1280-1282 (1998).
7. Nilsson, R., *Konstruktion och test av en externkavitetsdiodlaser med snabb frekvensavstämning*, (Lund reports on atomic physics, LRAP-241, Lund, Sweden, 1998).
8. Wieman, C. E. & Hollberg, L., Using Diode-Lasers For Atomic Physics, *Review of Scientific Instruments* **62**, 1-20 (1991).
9. Ricci, L. *et al.*, A Compact Grating-Stabilized Diode-Laser System For Atomic Physics, *Optics Communications* **117**, 541-549 (1995).
10. Casey, H. C., Sell, D. D. & Panish, M. B., Refractive index of Al_xGa_{1-x}As between 1.2 and 1.8 eV, *Applied Physics Letters* **24**, 63-65 (1974).
11. Kaminov, I. P., Eisenstein, G. & Stulz, L. W., Measurement of the modal reflectivity of an antireflection coating on a superluminescent diode, *IEEE Journal of Quantum Electronics* **19**, 493-495 (1983).
12. Fey-den Boer, A. C., Beijerinck, H. C. W. & van Leeuwen, K. A. H., High-power broad-area diode lasers for laser cooling, *Applied Physics B-Lasers and Optics* **64**, 415-417 (1997).
13. Gehrig, E., Beier, B., Boller, K. J. & Wallenstein, R., Experimental characterization and numerical modelling of an AlGaAs oscillator broad area double pass amplifier system, *Applied Physics B-Lasers and Optics* **66**, 287-293 (1998).
14. Casperson, J. M., Moore, F. G. & Casperson, L. W., Double-pass high-gain laser amplifiers, *Journal of Applied Physics* **86**, 2967-2973 (1999).
15. Gehrig, E., Hess, O. & Wallenstein, R., Modeling (sic!) of the performance of high-power diode amplifier systems with an optothermal microscopic spatio-temporal theory, *IEEE Journal of Quantum Electronics* **35**, 320-331 (1999).
16. Arnold, A. S., Wilson, J. S. & Boshier, M. G., A simple extended-cavity diode laser, *Review of Scientific Instruments* **69**, 1236-1239 (1998).
17. Loewen, E. G., Neviere, M. & Maystre, D., Grating efficiency theory as it applies to blazed and holographic gratings, *Applied Optics* **16**, 2711-2721 (1977).
18. Bengtsson, J. & Kauranen, P., *Konstruktion av temperaturregulator*, (Lund reports on atomic physics, LRAP-146, Lund, Sweden, 1993).
19. Bond, W. L., Measurement of the Refractive Indices of Several Crystals, *Journal of Applied Physics* **36**, 1674-1677 (1965).
20. Denton, R. T., Chen, F. S. & Ballman, A. A., Lithium tantalate light modulators, *Journal of Applied Physics* **38**, 1611-1617 (1967).

21. Fowler, V. J. & Schlafer, J., A Survey of Laser Beam Deflection Techniques, *Applied Optics* **5**, 1675-1682 (1966).
22. Fowler, V. J., Buhrer, C. F. & Bloom, L. R., Electro-optic light beam deflector, *Proceedings of the IEEE* **52**, 193-194 (1964).